

Amplifying higher-order sidebands in optomechanical transparency with gain and loss

Yafeng Jiao^{1,*}, Hao Lü^{2,3,*}, Jun Qian^{2,†}, Y. Li⁴, and H. Jing^{1,2,†}

¹Department of Physics, Henan Normal University, Xinxiang 453007, China

²Key Laboratory for Quantum Optics, Shanghai Institute of Optics and Fine Mechanics, Chinese Academy of Science, Shanghai 201800, China

³University of Chinese Academy of Sciences, Beijing 100049, China

⁴Beijing Computational Science Research Center, Beijing 100084, China

*These authors contributed equally to this work.

†Authors to whom any correspondence should be addressed.

E-mail: jqian@siom.ac.cn, jinghui73@foxmail.com

Abstract. We study the gain-enhanced nonlinear optomechanically-induced transparency (OMIT). We find that (i) for a single cavity, significant enhancement can be achieved for gain-assisted higher-order sidebands, including the transmission rate and the group delay; (ii) for active-passive-coupled cavities, in the vicinity of the gain-loss balance, hundreds of microsecond of relative delay or advance are attainable between the probe and the nonlinear sideband pulses. The gain-enhanced higher-order OMIT effects, as firstly revealed here, indicate the possibility to make a two-color modulator, which can control both the strength and group delay of not only the probe light but also its higher-order sidebands.

PACS numbers: 42.50.Wk, 03.65.Ta

1. Introduction

Cavity optomechanics (COM), based on radiation-pressure-induced coherent photon-phonon coupling, have led to many important advances in recent years [2, 3], e.g., ultra-weak force measurement [4–7], ground-state mechanical cooling [8, 9], phonon lasing [10, 11], and single-photon transporting [12] or quantum phonon squeezing [13]. A particularly relevant example to our work here is the optomechanically-induced transparency (OMIT), which as an analogue of electromagnetically-induced transparency in atomic systems [14–16], was proposed [17] and then demonstrated in experiments [18, 19]. In view of nonlinear nature of the COM interaction, OMIT not only provides a new way to store light in solid-state devices [20–23], but also leads to a variety of exotic nonlinear effects [24–28]. As a notable result of nonlinear OMIT process [29–33], higher-order sideband effects were studied for a single passive cavity [29, 34–36] where, however, the sideband signal is much weaker in comparison with the probe field. The tunability of higher-order sidebands, as well as the associated slow-light effect, have not yet been studied before.

In parallel with the advances in COM, parity-time(PT)-symmetric phase transition [37, 38] has also been observed recently in coupled optical microresonators [39], opening up novel applications such as low-power optical diodes [39, 40], single-mode lasing [41, 42], and other unconventional optical effects [43, 44]. Combining these two fields leads to new PT-assisted hybrid COM devices, revealing unique effects such as PT-symmetric phonon lasing [11] and PT-broken chaos [45]. An inverted OMIT spectrum, i.e. a non-amplifying dip in the otherwise strongly amplifying region, was also identified in the linear process for such a hybrid system [46] (for similar effects in a purely optical experiment, see Ref. [47]).

Inspired by the works mentioned above, here we study the nonlinear OMIT process and particularly the higher-order sidebands in a single active cavity or active-passive-coupled resonators. We show that (i) the second-order sideband exhibits an inverted-OMIT profile in both cases, in particular, the transmission of the second-order sideband pulse can be significantly enhanced in the vicinity of gain-loss balance; (ii) the group delay of second-order sideband pulses shows a strong dependence on the optical pump power, and the relative delay or advance between the probe and the nonlinear sideband pulses can be well adjusted within several hundreds of microsecond.

These results indicate the possibility to engineer the group velocities of different sideband pulses in OMIT process simultaneously, which is absent in previous studies. Also we note that the gain-enhanced nonlinear OMIT effect, as we studied here, is very different from the well-known slow or fast light phenomena by virtue of electromagnetically-induced transparency [16] or gain doublet effects [48] in atomic systems, in which only the signal pulse itself is generally controlled. As far as we know, the group delay of nonlinear second-order sideband and the tunable relative delay or advance between different sideband pulses have not been investigated in previous literatures.

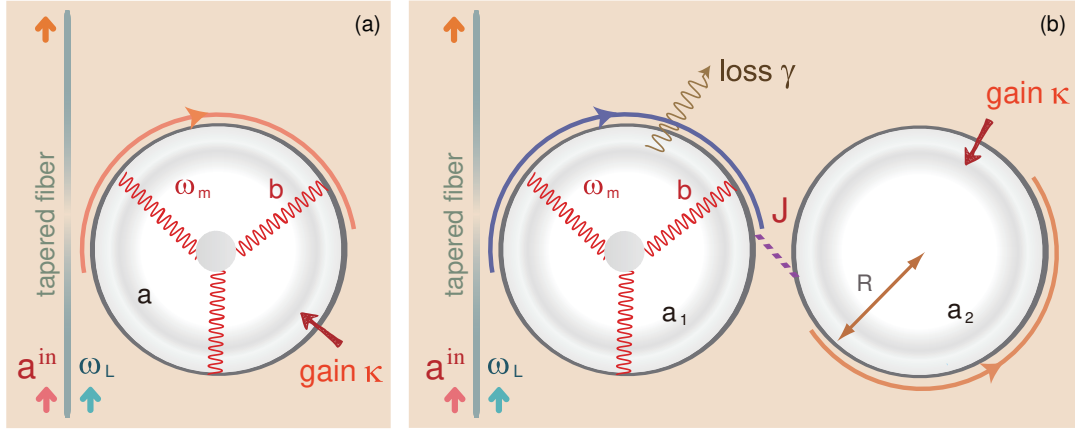


Figure 1. (Color online) Schematic of COM in a single active cavity (a) or an active-passive compound structure (b). In (b), the left cavity with an optical decay rate γ is coupled with a tapered fiber, and the right cavity with an optical gain κ [39, 46] is coupled to the left cavity with an optical tunneling rate J . In both cases, only the cavity coupled to the fiber supports a mechanical mode at frequency ω_m and is driven by a pump field at frequency ω_L .

This paper is organized as follows. In Sec. 2, we present the OMIT models for both a single active cavity and an active-passive compound system, with which to calculate the optical spectral responses and the associated group delays of both the probe field and the second-order sideband. Then in Sec. 3, we analyze in details the results of optical transmissions rates and group delays in a single cavity or an active-passive compound system, respectively, focusing on the important roles of the pump power and the gain-to-loss ratio. Finally in Sec. 4, we conclude with a brief discussion of the results presented in this work and an outlook of our future works.

2. Theoretical Model

As shown in Fig. 1, for possible comparisons, we consider two different setups consisting of a single active optomechanical cavity [49] and an active-passive compound structure, respectively. In both cases, the cavity-mode resonance frequency is ω_c , the cavity coupled with the tapered fiber contains a mechanical mode (with the effective mass m and the damping rate Γ_m) [10], and the COM coupling strength is denoted by g . As in Ref. [39], the active resonator, fabricated from Er^{3+} -doped silica, can emit photons in the 1550 nm band, when driven by a laser in the 980 nm or 1450 nm bands. In Fig. 1(a), we first focus on the gain-assisted OMIT in a single cavity, including the second-order transmission rate and the associated group delay. In Fig. 1(b), we turn to study the enhancement of the second-order sideband in the vicinity of gain-loss balance in a compound structure. Note that only the photons at the emission band of 1550 nm can tunnel through the air gap between the resonators, which provides an optical gain κ to compensate the optical loss γ in the passive resonator [39]. To observe the OMIT phenomenon, the optomechanical cavity is driven by both a strong pump laser at frequency ω_L and a weak

probe light at frequency ω_p , with the amplitudes $\varepsilon_l = \sqrt{\frac{2\gamma P_l}{\hbar\omega_l}}$, $\varepsilon_p = \sqrt{\frac{2\gamma P_{in}}{\hbar\omega_p}}$, respectively, where P_l and P_{in} denote the powers of the control and probe lasers. We are interested in the role of nonlinear COM interactions on the optical responses of the systems, particularly the relative group delay or advance of the probe light and the higher-order sideband pulse. Passive COM setups with single and compound cavities have been extensively investigated in theory and experiments in the past years. However, the study of optomechanical effects with active optomechanics are still in early stages [49], and the effects of gain-assisted optomechanical nonlinearity on high-order OMIT have been little studied.

2.1. Active nonlinear OMIT in a single cavity

As illustrated in Fig. 1(a), we study the transmission rates of the probe field and the second-order sideband in a single active optomechanical cavity [49]. The Hamiltonian of the system can be written at the simplest level as

$$H_1 = \hbar\Delta_l a^\dagger a + \frac{p^2}{2m} + \frac{1}{2}m\omega_m^2 x^2 - \hbar g a^\dagger a x + i\hbar (\varepsilon_l a^\dagger + \varepsilon_p a^\dagger e^{-i\xi t} - h.c.), \quad (1)$$

with the optical operator a and the mechanical position or momentum operator x or p , and the cavity-pump detuning and the probe-pump detuning, respectively, $\Delta_l \equiv \omega_c - \omega_l$, $\xi \equiv \omega_p - \omega_l$.

The Heisenberg equations of motion of this system are then

$$\begin{aligned} \ddot{x} + \Gamma_m \dot{x} + \omega_m^2 x - \frac{\hbar g}{m} a^\dagger a &= 0, \\ \dot{a} + (i\Delta_l - igx - \kappa)a - \varepsilon_l &= \varepsilon_p e^{-i\xi t}. \end{aligned} \quad (2)$$

The optical or mechanical gain and damping terms are added phenomenologically into the Eq. (2) [11,45]. Setting all the derivatives as zero leads to the steady-state values

$$x_s = \frac{\hbar g}{m\omega_m^2} |a_s|^2, \quad a_s = \frac{\varepsilon_l}{-\kappa + i\Delta_l - igx_s}. \quad (3)$$

All the operators are then divided into their stationary values and the remaining fluctuations, i.e. $x = x_s + \delta x$, $a = a_s + \delta a$, and the equations satisfied by the fluctuation terms are

$$\begin{aligned} \delta\ddot{x} + \Gamma_m \delta\dot{x} + \omega_m^2 \delta x - \frac{\hbar g}{m} (a_s \delta a^\dagger + a_s^* \delta a + \delta a^\dagger \delta a) &= 0, \\ \delta\dot{a} + (i\Delta_l - igx_s - \kappa)\delta a - ig(a_s \delta x + \delta x \delta a) &= 0. \end{aligned} \quad (4)$$

Here the second-order nonlinear terms such as $\delta x \delta a$ and $\delta a^\dagger \delta a$ are preserved in Eq. (4). Now we solve these equations by using the ansatz

$$\begin{aligned} \delta a &= A_+^{(1)} e^{-i\xi t} + A_-^{(1)} e^{i\xi t} + A_+^{(2)} e^{-2i\xi t} + A_-^{(2)} e^{2i\xi t}, \\ \delta x &= X^{(1)} e^{-i\xi t} + X^{(1)*} e^{i\xi t} + X^{(2)} e^{-2i\xi t} + X^{(2)*} e^{2i\xi t}. \end{aligned} \quad (5)$$

Substituting Eq. (5) into Eq. (4), and first neglecting the second-order parts in Eq. (5), leads to the linear response of the system

$$\begin{aligned} A_+^{(1)} &= \frac{[\lambda(\xi)\lambda_{s2}(\xi) + i\hbar g^2|a_s|^2]\varepsilon_p}{\lambda(\xi)\lambda_{s1}(\xi)\lambda_{s2}(\xi) + i[\lambda_{s1}(\xi) - \lambda_{s2}(\xi)]\hbar g^2|a_s|^2}, \\ X^{(1)} &= \frac{\lambda_{s2}(\xi)\hbar g a_s^* \varepsilon_p}{\lambda(\xi)\lambda_{s1}(\xi)\lambda_{s2}(\xi) + i[\lambda_{s1}(\xi) - \lambda_{s2}(\xi)]\hbar g^2|a_s|^2}, \end{aligned} \quad (6)$$

where

$$\lambda(\xi) = m(\omega_m^2 - \xi^2 - i\xi\Gamma_m), \quad \lambda_{s1,s2}(\xi) = -i\xi - \kappa \pm (i\Delta_l - igx_s). \quad (7)$$

Combining Eqs. (4)-(6) gives the second-order sideband amplitude

$$A_+^{(2)} = \frac{C_1 X^{(1)2} + C_2 A_+^{(1)} X^{(1)}}{\lambda_{s2}(\xi)[\lambda(2\xi)\lambda_{s1}(2\xi)\lambda_{s2}(2\xi) + i(\lambda_{s1}(2\xi) - \lambda_{s2}(2\xi))\hbar g^2|a_s|^2]} \quad (8)$$

where

$$\begin{aligned} C_1 &= -i\hbar g^4 a_s |a_s|^2, \\ C_2 &= \hbar g^3 (\lambda_{s2}(2\xi) - \lambda_{s2}(\xi)) |a_s|^2 + ig\lambda_{s2}(\xi)\lambda(2\xi)\lambda_{s2}(2\xi). \end{aligned} \quad (9)$$

We note that $A_+^{(2)}$, being proportional to ε_p^2 , is indeed smaller than the first-order term $A_+^{(1)}$ for a weak probe light. The first term or the second term of $A_+^{(2)}$ denotes an unconverted-like process of the pump light or the first-order sideband, respectively [29].

2.2. Nonlinear OMIT in active-passive-coupled resonators

Now we use the similar strategy as in the above derivations to treat the compound COM system as shown in Fig. 1(b). Including two optical modes $a_{1,2}$ and the mechanical mode containing now in the passive resonator, we write the Hamiltonian of this three-mode COM system as

$$H_2 = H_1 + \hbar\Delta_l a_2^\dagger a_2 - \hbar J(a_1^\dagger a_2 + a_2^\dagger a_1), \quad (10)$$

where for the expression of H_1 , we have used the replacement $a \rightarrow a_1$. The Heisenberg equations of this compound system are

$$\begin{aligned} \ddot{x} &= -\Gamma_m \dot{x} - \omega_m^2 x + \frac{\hbar g}{m} a_1^\dagger a_1, \\ \dot{a}_1 &= (-i\Delta_l + igx - \gamma)a_1 + iJa_2 + \varepsilon_l + \varepsilon_p e^{-i\xi t}, \\ \dot{a}_2 &= (-i\Delta_l + \kappa)a_2 + iJa_1. \end{aligned} \quad (11)$$

Expanding the operators as follows

$$\begin{aligned} a_1 &= a_{1,s} + A_{1+}^{(1)} e^{-i\xi t} + A_{1-}^{(1)} e^{i\xi t} + A_{1+}^{(2)} e^{-2i\xi t} + A_{1-}^{(2)} e^{2i\xi t}, \\ a_2 &= a_{2,s} + A_{2+}^{(1)} e^{-i\xi t} + A_{2-}^{(1)} e^{i\xi t} + A_{2+}^{(2)} e^{-2i\xi t} + A_{2-}^{(2)} e^{2i\xi t}, \\ x &= x_s + X^{(1)} e^{-i\xi t} + X^{(1)*} e^{i\xi t} + X^{(2)} e^{-2i\xi t} + X^{(2)*} e^{2i\xi t}, \end{aligned} \quad (12)$$

where $a_{i,s}$ ($i = 1, 2$) and x_s denotes the steady values, leads to the amplitude of the first-order sideband $A_{1+}^{(1)}$ and $X^{(1)}$, as given in Ref. [46], and also the second-order sideband

amplitude $A_{1+}^{(2)}$. We find that it has exactly the same form as the single-cavity result, i.e. the Eq. (8), but with the following replacements $a \rightarrow a_1$, $A_+^{(1)} \rightarrow A_{1+}^{(1)}$, $\lambda_{s1} \rightarrow \lambda_{d1}$, $\lambda_{s2} \rightarrow \lambda_{d2}$ with $\lambda_{d1,d2}(\xi) \equiv -i\xi + \gamma \pm \left(i\Delta_l - igx_s + \frac{J^2}{i\Delta_l - i\xi - \kappa} \right)$.

In both cases, the expectation value of the output field can be obtained by using the standard input-output relation, i.e. $a_1^{out} = a_1^{in} - \sqrt{\gamma}a_1$, where a_1^{in} and a_1^{out} are the input and output field operators, respectively. The transmitted rate of the probe light [46] and the efficiency of the second-order sideband (i.e. the ratio of the amplitude of the output second-order sideband to the amplitude of the input probe light) [29] are then defined by

$$|t_p|^2 = \left| \frac{a_1^{out}}{a_1^{in}} \right|^2 = \left| 1 - \frac{\gamma}{\varepsilon_p} A_{1+}^{(1)} \right|^2, \quad \eta = \left| \frac{\gamma}{\varepsilon_p} A_{1+}^{(2)} \right|,$$

respectively. In addition, the group delay of the probe light or the second-order sideband can be given by

$$\tau_g = \frac{d \arg(t_p)}{d\xi} \Big|_{\xi=\omega_m}, \quad \tau'_g = \frac{d \arg(A_{1+}^{(2)})}{d\omega} \Big|_{\xi=\omega_m} = \frac{d \arg(A_{1+}^{(2)})}{2d\xi} \Big|_{\xi=\omega_m},$$

respectively, taking into account of the second-order sideband frequency $\omega = 2\xi + \omega_l$. In the following, to illustrate the gain-assisted nonlinear OMIT effects, we choose the experimentally accessible parameters in our calculations, i.e. $\varepsilon_p/\varepsilon_l = 0.05$, (the radius of the resonators) $R = \omega_c/g = 34.5\mu\text{m}$, $m = 50 \text{ ng}$, $\omega_c = 1.93 \times 10^5 \text{ GHz}$, $\omega_m = 2\pi \times 23.4 \text{ MHz}$, $\gamma = 6.43 \text{ MHz}$ and $\Gamma_m = 2.4 \times 10^5 \text{ kHz}$. We set $\Delta_l = \omega_c - \omega_l = \omega_m$ and then we have $\Delta_p \equiv \omega_p - \omega_c = \xi - \omega_m$. In the single cavity case, we compare the active OMIT and the familiar passive OMIT results, where a negative $\kappa < 0$ indicates a passive cavity; while in the double-resonator case, we focus on the different features of the second-order sideband in the PT-symmetric and the PT-broken regimes, by tuning the gain-to-loss ratio κ/γ .

3. Results and discussions

3.1. Single-cavity case

We first discuss the OMIT and second-order sideband in the single active-cavity configuration. Fig. 2 shows the results of $|t_p|^2$ and η as a function of Δ_p . For comparison, we also plot the results in a passive cavity [29]. We find that, in sharp contrast to the conventional OMIT profile in a lossy cavity, an inverted-OMIT profile is obviously visible for the probe field in an active cavity (see Fig. 2(a)), characterizing a non-amplifying dip in the otherwise strongly amplifying region. This feature was also observed in the active-passive compound system [46,47]. However, this inverted feature does not exist in the second-order sideband process. As shown in Fig. 2(b), a double-peak structure in the transmission spectrum can be seen in both cases of passive and active COM systems. This indicates that by using an active cavity, one can simultaneously amplify the weak probe field and the sideband signal. This, again, is distinct from that in a passive COM

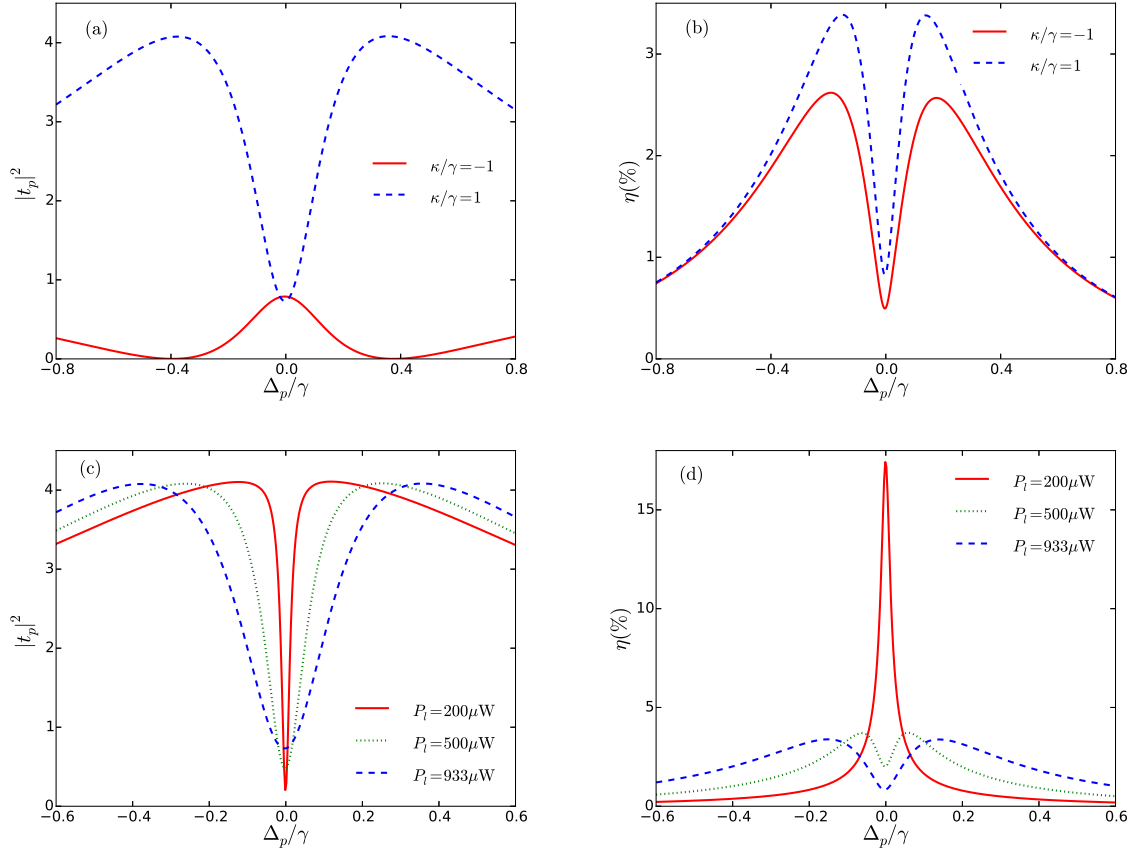


Figure 2. Transmission of the probe light $|t_p|^2$ (a,c) and the efficiency of the second-order sideband process η (b,d) vary with the ratio κ/γ and the pump power P_l in the case of the single cavity. The pump power is fixed as $P_l = 933\mu\text{W}$ in (a) and (b), while $\kappa/\gamma = 1$ is chosen in (c) and (d).

system, where the generation of the second-order sideband tends to be suppressed in the transmission window of the probe field [29]. In Fig. 2(c,d), we give the dependences of the probe field and the second-order sideband on the driving power P_l for $\kappa > 0$. We see that these two processes are complementary at the resonance $\Delta_p = 0$: with decreasing P_l from $933\mu\text{W}$ to $200\mu\text{W}$, the transmission rate of the probe field is slightly decreased, which results in a significant increasing of the second-sideband efficiency at $\Delta_p = 0$.

Fig. 3(a) shows the group delay of the generated up-converted sideband signal at different pumping powers in such an active COM system. For a conventional lossy cavity, the group delay of the second-order sideband has only changed in a small range of $\sim 2\mu\text{s}$, while for the active COM setup it experiences a remarkable slow-to-fast light transition at $P_l \sim 0.12\text{mW}$, where τ'_g varies within a substantial range between $\pm 200\mu\text{s}$. Furthermore, the relative delay between the transmitted probe and the generated sideband signals, $\Delta\tau_g = \tau_g - \tau'_g$, can be calculated for both cases of $\kappa > 0$ and $\kappa < 0$ (see Fig. 3(b)). We see that in the passive COM, $\Delta\tau_g > 0$, i.e. the probe field always travels behind the associated second-order sideband signal. However, the relative delay ($\sim 4\mu\text{s}$)

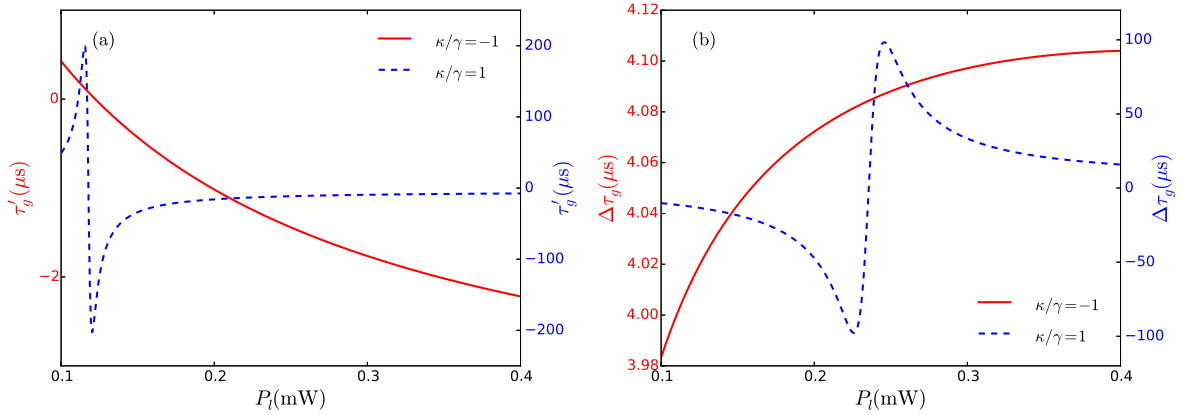


Figure 3. (a) Group delay or advance of the second-order sideband at the resonance $\Delta_p = 0$, as a function of pump power for a single passive ($\kappa/\gamma = -1$) or an active cavity ($\kappa/\gamma = 1$). (b) Relative group delay $\Delta\tau_g = \tau_g - \tau_g'$ between the probe and second-order sideband fields.

is almost unchanged within a wide range of P_l , which is not beneficial for their separation in the time domain. In contrast, for the active COM system, the gain-assisted fast light can be observed for both the probe field and the second-order output signal, and the delay or advance can be significantly amplified by tuning κ and P_l . The maximum value of $\Delta\tau_g$ can be improved for about 25 times, in a similar range of P_l . Even the sign of $\Delta\tau_g$ can be reversed to negative at lower pump power, i.e. the second-order signal can also travel behind the probe field, which is strikingly distinct from the passive COM situation. This feature holds the promise to be useful for making e.g. a low-power modulator both in frequency and time domains.

3.2. Coupled cavities with gain-loss balance

Now we probe the nonlinear OMIT in active-passive-coupled resonators (see Fig. 1(b)). First, as shown in Figs. 4(a), we give the efficiency of the second-order sideband for different values of $\kappa > 0$. We find that for the off-resonance case $\Delta_p \neq 0$, the second-order profile shows an interesting similarity to the first-order case: the field amplification tends to be maximized as the gain and loss approach to the balance ($\kappa/\gamma = 1$), and the reversed-gain dependence works for both of the two processes. In order to receive some analytical estimations, we take $\omega_m/\omega_c \sim 0$, $x_s \sim 0$, which approximately leads to

$$\eta \approx \left| \frac{i\hbar^2 g^4 |a_{1,s}|^2 a_{1,s}^* \kappa^4 \gamma \varepsilon_p}{2m^2 \Gamma_m^2 \omega_m^3 (J^2 - \kappa\gamma)^3 [m\omega_m \Gamma_m (J^2 - \kappa\gamma) + i\hbar g^2 |a_{1,s}|^2 (J^2 - \kappa^2)]} \right|. \quad (13)$$

Obviously, in the vicinity of the gain-loss balance ($\kappa/\gamma = 1$, $J/\gamma = 1$), the efficiency of second-order sideband generation is most preferable. We also note that, at the resonance $\Delta_p = 0$, η is maximized for $\kappa/\gamma \sim 0.12$ (see Fig.4(b)), much large than that in a passive COM system.

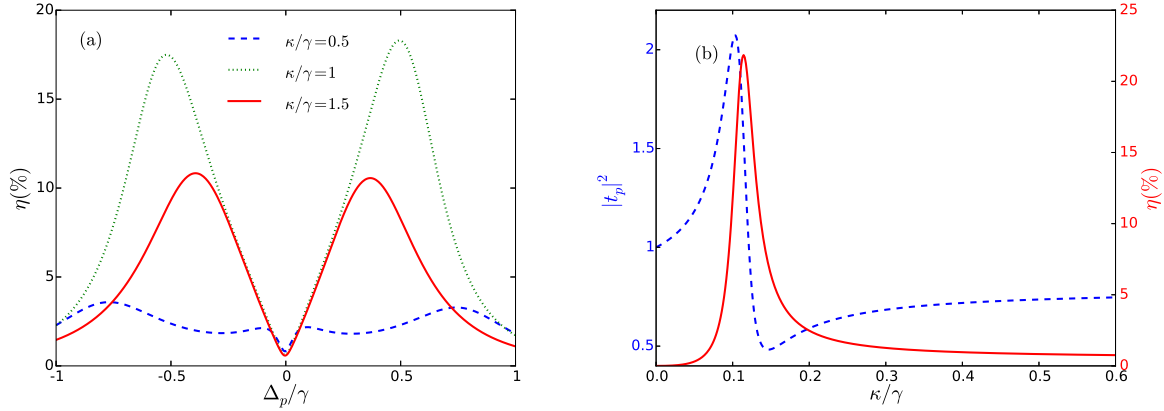


Figure 4. (a) Transmission spectra of the second-order sideband in an active-passive compound system, for $\kappa/\gamma = 0.5$ (blue dashed), 1.0 (green dotted) and 1.5 (red solid). (b) $|t_p|^2$ (blue dashed) and η (red solid) at the resonance $\Delta_p = 0$, as a function of the gain-to-loss ratio κ/γ . In all the figures we have taken $J/\gamma = 1$ and $P_l = 933 \mu\text{W}$.

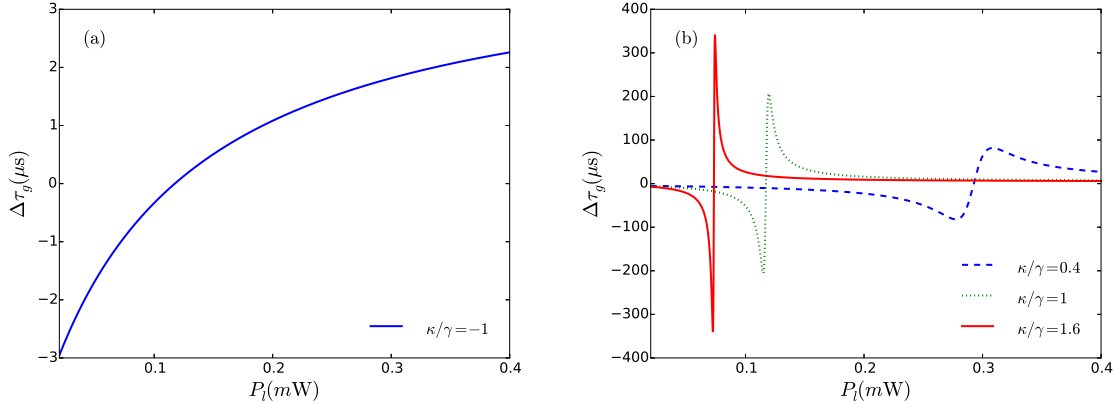


Figure 5. The relative group delay $\Delta\tau_g$ as a function of P_l for the passive-passive system ($\kappa/\gamma = -1$) (a) or the active-passive system, with $\kappa/\gamma = 0.4$ (blue dashed), 1.0 (green dotted) and 1.6 (red solid) (b). Other parameters are $\Delta_p = 0$ and $J/\gamma = 1$.

We have also studied the role of the optical tunneling rate J on both $|t_p|^2$ and η , at the resonance $\Delta_p = 0$. For $J/\gamma \rightarrow 0$, the compound system is reduced to the passive single-cavity system. We find that for the passive-passive system, stronger tunneling J is favorable for the first-order process (but not for the second-order process) [29]; in contrast, for the active-passive system, stronger tunneling J is favorable for the second-order process. Finally, the relative delay between the probe and sideband fields is shown in Fig. 5; for the gain-assisted advance of the probe field, see Ref. [46]. For a passive-passive system ($\kappa/\gamma = -1$), $\Delta\tau_g$ only changes within the scope of several microseconds. In contrast, drastic changes of $\Delta\tau_g$ from delay to advance can be seen in the active-passive COM system, for example, up to $\pm 100 \mu\text{s}$ can be achieved for $\kappa/\gamma = 0.4$, indicating the ability to flexibly modulate the nonlinear responses of the COM system,

particularly in the vicinity of gain-loss balance.

4. Conclusion

In summary, we have studied unconventional effects in the gain-assisted nonlinear OMIT, including the inverted-OMIT spectrum for the second-order sideband and the tunable relative delay or advance of the probe and the sideband fields. We note that, for a single cavity, gain-enhanced optomechanical cooling was recently revealed [49], but the associated OMIT effects, i.e. the optical transparency or the group delay, was not yet studied. We also note that in COM, coupled resonators can possess several advantages in comparison with the single cavity [11, 45]. The previous work on active OMIT was limited to the linear process in coupled resonators [45]; hence our work here enables direct comparisons not only between the single-cavity and double-cavity cases, but also between the linear and nonlinear OMIT effects.

In comparison with an acousto-optical modulator (AOM) which is commonly used in frequency shift of a laser beam, the active COM device can also generate a frequency-shifted sideband similar to the AOM, but with an additional ability to separate it with the input signal pulse in timing sequence by tuning their relative group delay or advance. The practical application of active OMIT effects in e.g. optical frequency shifter or filter, however, is beyond the purpose of our work here and certainly deserves further studies. In the future, we also plan to study nonlinear OMIT in a cascaded system with two mechanical modes [23], in a hybrid COM system [12], or in an active COM system with a spin defect [50].

Acknowledgements

We thank Xin-You Lü for helpful discussions. This work is supported partially by the CAS 100-Talent program and the National Natural Science Foundation of China under Grant numbers 11274098, 11474087, and 11422437.

References

- [1] Aspelmeyer M, Kippenberg T J and Marquardt F 2014 *Rev. Mod. Phys.* **86** 1391.
- [2] Aspelmeyer M, Meystre P and Schwab K 2012 *Phys. Today* **65** 29
- [3] Metcalfe M 2014 *App. Phys. Rev.* **1** 031105
- [4] Dobrindt J M, Wilson-Rae I and Kippenberg T J 2008 *Phys. Rev. Lett.* **101** 263602
- [5] Gröblacher S, Hammerer K, Vanner M R and Aspelmeyer M 2009 *Nature* **460** 724
- [6] Arcizet O, Cohadon P F, Briant T, Pinard M, Heidmann A, Mackowski J M, Michel C, Pinard L, François O and Rousseau L 2006 *Phys. Rev. Lett.* **97** 133601
- [7] Teufel J D, Donner T, Castellanos-Beltran M A, Harlow J M and Lehnert K M. 2009 *Nat. Nanotech.* **4** 820
- [8] Teufel J D, Donner T, Li D, Harlow J W, Allman M S, Cicak K, Sirois A J, Whittaker J D, Lehnert K M and R W Simmonds 2011 *Nature* **475** 359
- [9] Chan J, Mayer Alegre T P, Safavi-Naeini A H, Hill J T, Krause A, Gröblacher S, Aspelmeyer M and Painter O 2011 *Nature* **478** 89

- [10] Grudinin I S, Lee H, Painter O and Vahala K J 2010 *Phys. Rev. Lett.* **104** 083901
- [11] Jing H, Özdemir S K, Lü X Y, Zhang J, Yang L and Nori F 2014 *Phys. Rev. Lett.* **113** 053604
- [12] Jia W Z and Wang Z D 2013 *Phys. Rev. A* **88** 063821
- [13] Wollman E E, Lei C U, Weinstein A J, Suh J, Kronwald A, Marquardt F, Clerk A A and Schwab K C 2015 *Science* **349** 952
- [14] Boller K J, Imamoglu A and Harris S E 1991 *Phys. Rev. Lett.* **66** 2593
- [15] Lukin M D, Fleischhauer M, Scully M O and Velichansky V L 1998 *Opt. Lett.* **23** 295
- [16] Fleischhauer M, Imamoglu A and Marangos J P 2005 *Rev. Mod. Phys.* **77** 633
- [17] Agarwal G S and Huang S 2010 *Phys. Rev. A* **81** 041803
- [18] Weis S, Rivière R, Deleglise S, Gavartin E, Arcizet O, Schliesser A and Kippenberg T J 2010 *Science* **330** 1520
- [19] Safavi-Naeini A H, Alegre T P M, Chan J, Eichenfield M, Winger M, Lin Q, Hill J T, Chang D E and Painter O 2011 *Nature* **472** 69
- [20] Zhou X, Hocke F, Schliesser A, Marx A, Huebl H, Gross R and Kippenberg T J 2013 *Nat. Phys.* **9** 179
- [21] Chang D E, Safavi-Naeini A H, Hafezi M and Painter O 2011 *New J. Phys.* **13** 023003
- [22] Fiore V, Yang Y, Kuzyk M C, Barbour R, Tian L and Wang H 2011 *Phys. Rev. Lett.* **107** 133601
- [23] Fan L, Fong K Y, Poot M and Tang H X 2015 *Nat. Commun.* **6** 5850
- [24] Stannigel K, Komar P, Habraken S J M, Bennett S D, Lukin M D, Zoller P and Rabl P 2012 *Phys. Rev. Lett.* **109** 013603
- [25] Ludwig M, Safavi-Naeini A H, Painter O and Marquardt F 2012 *Phys. Rev. Lett.* **109** 063601
- [26] Basiri-Esfahani S, Akram U and Milburn G J 2012 *New J. Phys.* **14** 085017
- [27] Stannigel K, Rabl P, Sørensen A S, Lukin M D and Zoller P 2011 *Phys. Rev. A* **84** 042341
- [28] Nunnenkamp A, Børkje K and Girvin S M 2011 *Phys. Rev. Lett.* **107** 063602
- [29] Xiong H, Si L G, Zheng A S, Yang X and Wu Y 2012 *Phys. Rev. A* **86** 013815
- [30] Lemonde M A, Didier N and Clerk A A 2013 *Phys. Rev. Lett.* **111** 053602
- [31] Børkje K, Nunnenkamp A, Teufel J D and Girvin S M 2013 *Phys. Rev. Lett.* **111** 053603
- [32] Liu Y C, Xiao Y F, Chen Y L, Yu X C and Gong Q 2013 *Phys. Rev. Lett.* **111** 083601
- [33] Kronwald A and Marquardt F 2013 *Phys. Rev. Lett.* **111** 133601
- [34] Ma J, You C, Si L G, Xiong H, Li J, Yang X and Wu Y 2015 *Sci. Rep.* **5** 11278
- [35] Suzuki H, Brown E and Sterling R 2015 *Phys. Rev. A* **92** 033823
- [36] Ma P C, Zhang J Q, Xiao Y, Feng M and Zhang Z M 2014 *Phys. Rev. A* **90** 043825
- [37] Bender C M and Boettcher S 1998 *Phys. Rev. Lett.* **80** 5243
- [38] Bender C M, Gianfreda M, Özdemir S K, Peng B and Yang L 2013 *Phys. Rev. A* **88** 062111
- [39] Peng B, Özdemir S K, Lei F, Monifi F, Gianfreda M, Long G L, Fan S, Nori F, Bender C M and Yang L 2014 *Nat. Phys.* **10** 394
- [40] Chang L, Jiang X, Hua S, Yang C, Wen J, Jiang L, Li G, Wang G and Xiao M 2014 *Nat. Photon.* **8** 524
- [41] Feng L, Wong Z J, Ma R M, Wang Y and Zhang X 2014 *Science* **346** 972
- [42] Hodaei H, Miri M A, Heinrich M, Christodoulides D N and Khajavikhan M 2014 *Science* **346** 975
- [43] Peng B, Özdemir S K, Rotter S, Yilmaz H, Liertz M, Monifi F, Bender C M, Nori F and Yang L 2014 *Science* **346** 328
- [44] Wan W, Chong Y, Ge L, Noh H, Stone A D and Cao H 2011 *Science* **331** 889
- [45] Lü X Y, Jing H, Ma J Y and Wu Y 2015 *Phys. Rev. Lett.* **114** 253601
- [46] Jing H, Özdemir S K, Geng Z, Zhang J, Lü X Y, Peng B, Yang L and Nori F 2015 *Sci. Rep.* **5** 9663
- [47] Oishi T and Tomita M 2013 *Phys. Rev. A* **88** 013813
- [48] Wang L J, Kuzmich A and Dogariu A 2000 *Nature* **406** 277
- [49] Ge L, Faez S, Marquardt F and Türeci H E 2013 *Phys. Rev. A* **87** 053839
- [50] Ramos T, Sudhir V, Stannigel K, Zoller P and Kippenberg T J 2013 *Phys. Rev. Lett.* **110** 193602